Aalborg Universitet

A Robust Passive Damping Method for LLCL-Filter-Based Grid-Tied Inverters to Minimize the Effect of Grid Harmonic Voltages

Wu, Weimin; Sun, Yunjie; Huang, Min; Wang, Xiongfei; Wang, Huai; Blaabjerg, Frede; Liserre, Marco; Chung, Henry Shu-hung

A Robust Passive Damping Method for LLCL Filter Based Grid-Tied Inverters to Minimize the Effect of Grid Harmonic Voltages

Weimin Wu, Yunjie Sun, Min Huang, Xiongfei Wang, Huai Wang, Frede Blaabjerg, *Fellow, IEEE*, Marco Liserre, *Fellow, IEEE*, and Henry Shu-hung Chung, *Senior Member, IEEE*

Abstract- **In order to minimize the effect of the grid harmonic voltages, harmonic compensation is usually adopted for a grid-tied inverter. However, a large variation of the grid inductance challenges the system stability in case a high-order passive filter is used to connect an inverter to the grid. Although in theory, an adaptive controller can solve this problem, but in such case the grid inductance may need to be detected on-line, which will complicate the control system. This paper investigates the relationship between the maximum gain of the controller that still keeps the system stable and the *Q-factor* for a grid-tied inverter with an *RL* series or an *RC* parallel damped high-order power filter. Then, a robust passive damping method for *LLCL*-filter based grid-tied inverters is proposed, which effectively can suppress the possible resonances even if the grid inductance varies in a wide range. Simulation and experimental results are in good agreement with the theoretical analysis.**
Keywords: LLCL-filter; Passive damping; Grid-tied inverter; Q-factor; RC parallel damper; RL series damper; Robust.

I. INTRODUCTION

Driven by the shortage of fossil fuels, the renewable power generation technology receives an increased attention. The grid-tied Pulse Width Modulation (PWM) inverter has been widely used to connect the renewable energy with the utility grid [1]-[11]. The use of PWM scheme requires an output filter to limit the harmonic content of the grid-injected current, fulfilling the standards of IEEE 1547.2-2008 and IEEE 519-1992 [16], [17]. An *LCL*-filter is gaining more acceptances over an *L*-filter for the grid-tied Voltage Source Inverters (VSI) due to its smaller size, lower cost and better dynamics [18]. Recently, to further reduce the inductor size, a novel high-order power filter (*LLCL*-filter) has been proposed in [19].

In order to minimize the effect of the grid background harmonic voltages (e.g. 3th-9th), the Proportional Resonant plus Harmonic Compensation (*PR+HC*) controller has become a popular approach for the grid-tied inverters. However, a large variation of the grid inductance challenges the stability of the high-order power filter based system [20]. Although an adaptive controller can solve this problem in theory [21], the grid inductance may vary in a wide range, for example in a weak grid or a micro-grid. Thus, the performance of the adaptive controller is heavily dependent on the on-line information of the grid inductance, which complicates the controller design and operation.

It is well known that the passive damping method can improve the stability of system. An *RC* parallel damper is often adopted to reduce the power losses [22]. Nevertheless, this damping method can only take effect for the grid with a narrow variation of inductance [23]. For the grid inductance varying in a wide range, the design of a robust passive damper for a high

order power filter based grid-tied inverter still needs further research.

In this paper, both the upper and the lower limits of the *PR+HC* controller gain are first analyzed. Then, an equivalent *Q-factor* (*E-Q-factor*) calculation method is introduced to select the optimal passive damping parameters. On the basis of this, a robust passive damping scheme for the *LLCL*-filter based grid-tied inverters is proposed in order to overcome the adverse effect of the large grid inductance variation and to suppress the possible resonance. Finally, simulations and experimental results on a 2 kW single-phase grid-tied inverter prototype are presented to confirm the correctness of theoretical analysis.

II. UPPER AND LOWER LIMITS OF *PR+HC* CONTROLLER GAIN

When a *PR+HC* controller is adopted, the system open-loop gain, the control bandwidth and the system stability margin are determined by the proportional gain, k_p, of the controller [24]. In this section, the upper and the lower limits of k_p will be analyzed.

A. Configuration of the LLCL-Filter Based Grid-tied Inverter

Fig. 1 shows a typical grid-tied inverter with an *LLCL*-filter.
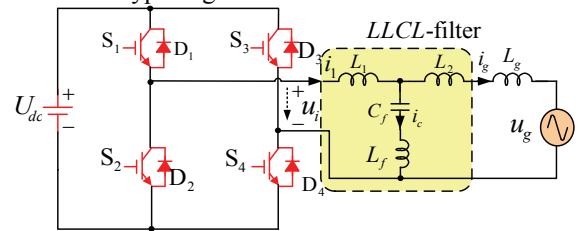
Fig.1. Voltage Source Inverter connected to the grid through an *LLCL*-filter [19].

The transfer function of the grid-injected current versus the output voltage of the inverter can be derived as

$$G_{u_i \to i_g}(s) = \frac{i_g(s)}{u_i(s)}\bigg|_{u_g(s)=0}$$
$$= \frac{L_f C_f s^2 + 1}{\left(L_1(L_2+L_g)C_f + \left(L_1+(L_2+L_g)\right)L_f C_f\right)s^3 + \left(L_1+(L_2+L_g)\right)s}$$

$$(1).$$

If L_f is set to zero, then the transfer functions $i_g(s)/u_i(s)$ of the classical *LCL*-filter can also be derived.

Fig. 2 shows the diagram of the system using the grid-side current feedback control, where $G_c(s)$ denotes the *PR+HC* controller, $H(s)$ is the sensor gain of the grid-injected current and $G_{inv}(s)$ is the gain of the PWM inverter.

This article has been accepted for publication in a future issue of this journal, but has not been fully edited. Content may change prior to final publication.

2

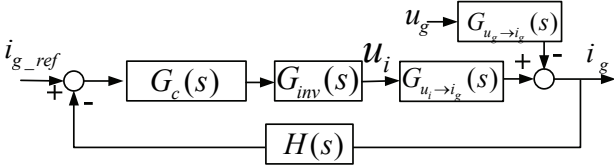**Fig. 2. Control block of system using the grid-side current as feedback.**

The open-loop transfer function of the system and the magnitude of the open-loop gain can be derived as follows,

$$G_{open-loop}(s) = G_c(s)G_{u_i \to i_g}(s)G_{inv}(s)H(s) \tag{2}$$

$$|G_{open-loop}(j\omega)| = 20\log|G_c(j\omega)G_{u_i \to i_g}(j\omega)G_{inv}(j\omega)H(j\omega)| \tag{3}$$

B. Lower Limit of PR+HC Controller Gain

In order to plug in the *PR+HC* controller, the crossover frequency should be larger or equal to a set value of f_{min_cross} under the weakest grid condition. In this paper, f_{min_cross} is designed as 500 Hz to suppress up to 9th harmonic currents. Since in the low frequency range, the *LCL*- or the *LLCL*-filter has approximately the same frequency characteristic as the *L*-filter and the loop gain has unity value at the cross-over frequency, the lower limit of the *PR+HC* controller gain can be derived as

$$k_{p\_min} = \frac{2\pi f_{min\_cross}(L_1 + L_2 + L_g)}{|G_{inv}(j2\pi f_{min\_cross})H(j2\pi f_{min\_cross})|} \tag{4}$$

C. Upper Limit of PR+HC Controller Gain

The derivation of the upper limit for the controller gain is organized into two steps. First, a conservative upper limit, $k_{p\_max\_1}$ can be derived based on the gain margin of the system open-loop transfer function. Then, considering the acceptable phase margin, the second upper limit $k_{p\_max\_2}$ can be obtained. As a consequence, the designed controller gain can be chosen as

$$k_{p\_min} \le k_p < \min\left(k_{p\_max\_1}, k_{p\_max\_2}\right) \tag{5}$$

Step 1: Controller gain based on the gain margin

For a conservative controller design under the different grid conditions, the open-loop gain $|G_{open-loop}(j\omega)|$ should be less than 0 dB whenever ω is larger than cross-over frequency in rad/s. Assuming that the transfer function of the grid-side current versus the output voltage of the inverter with a passive damped high-order filter is $G_{ui-ig}'(s, L_g)$, and thus the gain of the controlled plant $|G_{plant}'(j\omega)|$ can be given by

$$|G_{plant}'(j\omega)| = 20\log|G_{u_i \to i_g}'(j\omega)G_{inv}(j\omega)H(j\omega)| \tag{6}$$

Once the parameters of a passive damped high-order filter are chosen, $|G_{plant}'(j\omega)|$ is a function of ω and L_g. Its first-order partial derivative and Hessian matrix can be derived in equation (7) and (8) respectively,

$$\frac{\partial|G_{plant}'(j\omega, L_g)|}{\partial\omega} = 0$$

$$\frac{\partial|G_{plant}'(j\omega, L_g)|}{\partial L_g} = 0 \tag{7}$$

$$H_f = \begin{vmatrix} \dfrac{\partial^2|G_{plant}'(j\omega, L_g)|}{\partial\omega^2} & \dfrac{\partial^2|G_{plant}'(j\omega, L_g)|}{\partial L_g \partial\omega} \\ \dfrac{\partial^2|G_{plant}'(j\omega, L_g)|}{\partial\omega \partial L_g} & \dfrac{\partial^2|G_{plant}'(j\omega, L_g)|}{\partial L_g^2} \end{vmatrix} \tag{8}$$

From (7) and (8), the frequency ω_{max_1} and grid inductance $L_{g\_max\_1}$ corresponding to the local maximum gain of the plant can be calculated. And since the *PR+HC* controller is chosen, the conserved maximum gain of the controller can be derived as

$$k_{p\_max\_1} = \frac{1}{|G_{u_i \to i_g}'(j\omega_{max\_1}, L_{g\_max\_1})G_{inv}(j\omega_{max\_1})H(j\omega_{max\_1})|} \tag{9}$$

Step 2: Controller gain based on the phase margin

In the digital control system, the delay (T_d) that includes the control delay, sampling delay and PWM delay is inevitable, which compresses the phase margin of the open-loop transfer function. Thus, to preserve the system stability, the derived upper limit of the controller gain needs to keep the phase margin larger than a set value, PM_{min}, which can be given by

$$PM(\omega_{cross}) = \pi + \angle G_{u_i - i_g}'(j\omega_{cross}, L_g) - \omega_{cross} \cdot T_d$$

$$= \pi + \angle G_{u_i - i_g}'(j\omega_{cross}, L_g) - \frac{k_p \cdot |G_{in}(j\omega_{cross}) \cdot H(j\omega_{cross})|}{L_1 + L_2 + L_g} \cdot T_d$$

$$\ge PM_{min} \tag{10}$$

where, ω_{cross} is the cross-over frequency in Hz, and $\angle G_{u_i - i_g}'(j\omega, L_g)$ is the phase delay caused by $G_{u_i - i_g}'(j\omega, L_g)$. Hence, from (10), the maximum loop gain of $k_{p\_max\_2}$ can be determined based on the expected phase margin.

III. E-Q-FACTOR BASED PASSIVE DAMPING DESIGN

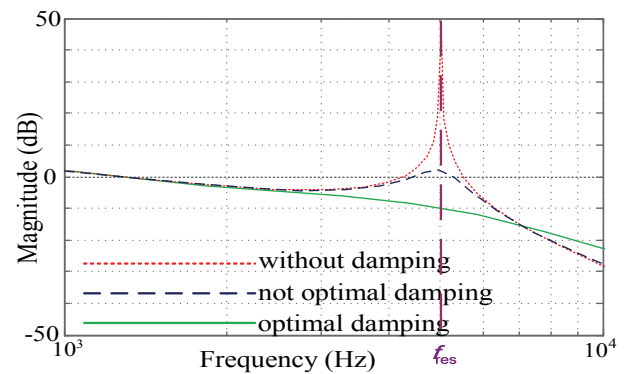#### A. Priciple of Equivalent Q-factor Method

Fig.3. Bode plots of the filter with different *Q-factor* values.

Fig. 3 shows the frequency responses of a high-order filter system without and with the passive damper. It is known that the passive damper aims to reduce the *Q-factor* at the dominant resonant frequency f_{res} in Hz. For a high-order filter based system, the optimized *Q-factor* is difficult to obtain by directly analyzing the complex conjugate solutions of the transfer function $G_{ui-ig}'(s, L_g)$, since the dominant resonance frequency varies with the different parameters [23]. However, in [23], it has also been pointed out that the *LLCL*-filter has almost the same frequency response as the *LCL*-filter within half of the

This article has been accepted for publication in a future issue of this journal, but has not been fully edited. Content may change prior to final publication.

3

switching frequency range.

Hence, similar to the *LCL*-filter, the *LLCL*-filter circuit can be simplified as a simple equivalent *LCR* series resonant circuit to calculate the equivalent *Q-factor* at the dominant resonance frequency. This method is named as *E-Q-factor* analysis and represented as

$$Q_E = \frac{1}{R_E}\sqrt{\frac{L_E}{C_E}}$$

(11)

where Q_E is the equivalent *Q-factor*, R_E, L_E and C_E are the equivalent resistor, inductance and capacitance of an equivalent series *LCR* circuit, respectively.

Three passive damped *LCL*- filter and *LLCL*-filter based systems and Bode diagrams of the grid-injected current versa the output voltage of the inverter are shown in Fig. 4, Fig. 5 and Fig. 6 respectively, where all the parameters are listed in Table I and the grid inductance is assumed to be zero. It can be further seen that the stability of *LCL*- filter or *LLCL*-filter based system is dependent on the dominant poles if the *PR+HC* controller is adopted. Compared with the *LCL*-filter, the *LLCL*-filter does not make extra troubles on the control of the whole inverter system.
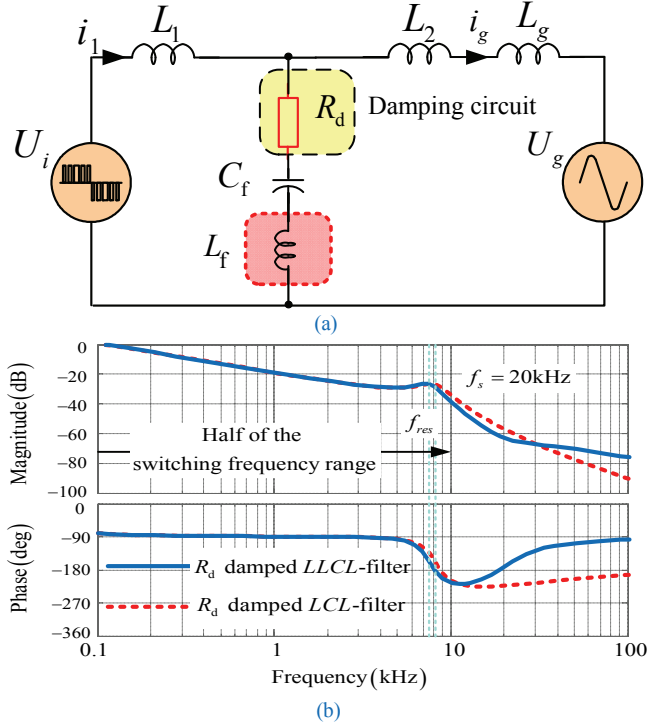

(a)

(b)

Fig. 4. Simply damped *LCL*- or *LLCL*-filter with R_d based inverter system: (a) topology, (b) Bode plots of transfer functions i_g (s) / u_i (s).
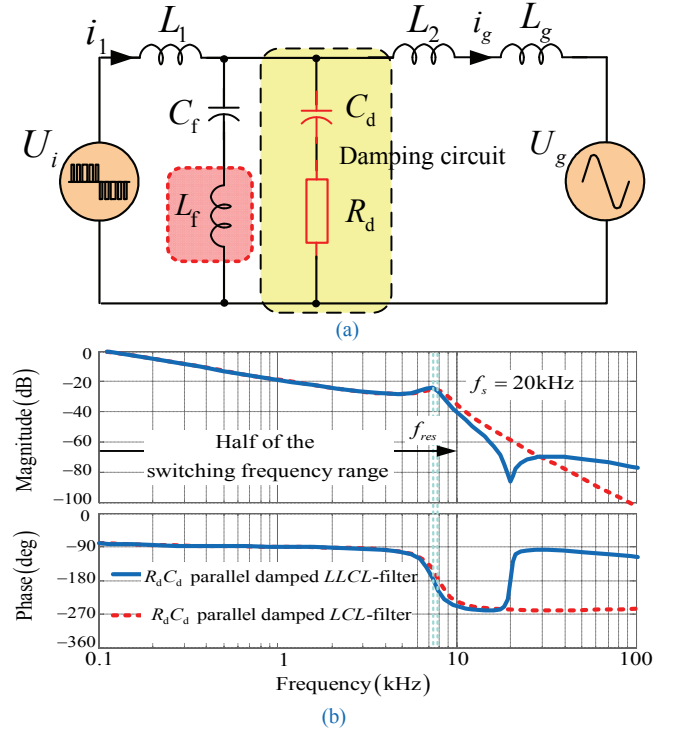

(a)

(b)

Fig. 5. *RC* parallel damped *LCL*- or *LLCL*-filter based inverter system: (a) topology, (b) Bode plots of transfer functions i_g(s) / u_i(s).
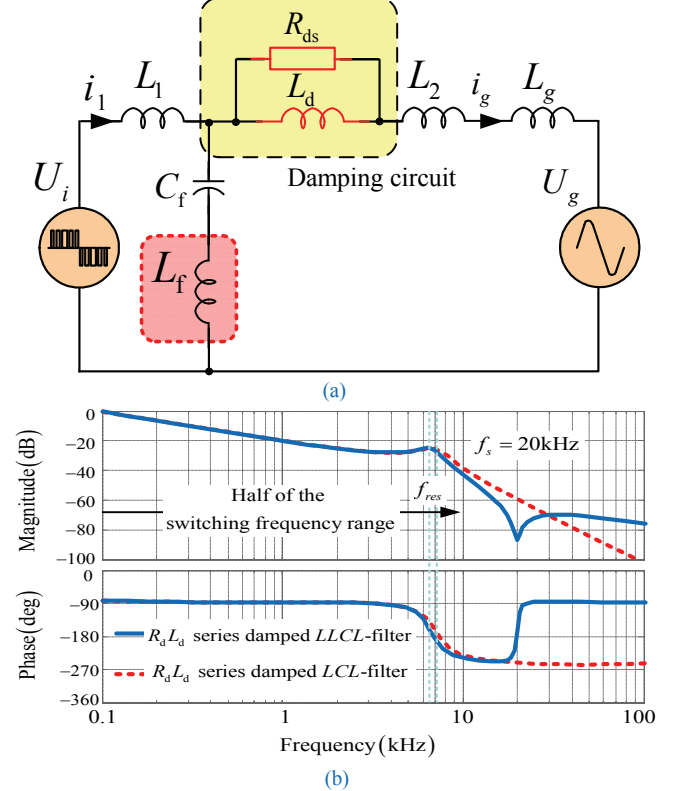

(a)

(b)

Fig. 6. *RL* series damped *LCL*- or *LLCL*-filter based inverter system: (a) topology, (b) Bode plots of transfer functions i_g (s) / u_i (s).

TABLE I PARAMETERS OF THREE PASSIVE DAMPED FILTERS

	Parameters of two filters				Parameters of dampers			
	LCL-filter	*LLCL*-filter	Parasitic resistance of the inductors			R_d damper	*RC* parallel damper	*RL* series damper	*Composite damper*
L_1	1.2 mH	1.2 mH	R_1	0.1 ohm	R_d	3 ohm	35 ohm	−	35 ohm
L_2	0.22 mH	0.22 mH	R_2	0.01 ohm	C_d	−	2 μF	−	2 μF
C_f	2 μF	2 μF	−	−	L_d	−	−	0.22 mH	0.22 mH
L_f	−	32 μH	R_f	0.2 ohm	R_{ds}	−	−	7 ohm	7 ohm

This article has been accepted for publication in a future issue of this journal, but has not been fully edited. Content may change prior to final publication.

4

where the resistors R_1, R_2 and R_f are the respective parasitic resistance of the inductors L_1, L_2 and L_f.

Based on (11), the calculated Q-factor of three passive damping methods are listed in table II if $L_g=0$.

TABLE II Q-factor of LCL-filter and $LLCL$-filter with three dampers

Q-factor of LCL-filter and $LLCL$-filter with three dampers			
	R_d damper	RC parallel damper	RL series damper
LCL-filter	3.214	3.978	3.603
$LLCL$-filter	3.479	3.742	4.102

B. E-Q-factor based RC parallel damping design

As shown in Fig. 5 (a), if the L_f is shortened, the diagram of the RC parallel damped LCL-filter can be obtained. The equivalent resistor R_E and capacitance C_E of the bypass capacitor C_f and the RC parallel damper can be calculated as,

$$\left.\frac{1}{sC_f}//(\frac{1}{sC_d}+R_d)\right|_{s=j\omega} = \left.\frac{R_dC_ds+1}{(R_dC_dC_fs^2+(C_d+C_f)s)}\right|_{s=j\omega} = R_E+\frac{1}{sC_E}$$

(12).

Then, at the dominant resonance frequency, the equivalent resistor R_E, inductance L_E and capacitance C_E of the equivalent LCR circuit can be calculated as

$$R_E = \left.\frac{R_dC_d^2}{(C_d+C_f)^2-(R_dC_dC_fs)^2}\right|_{s=j\cdot2\pi f_{res}}$$

$$L_E = \frac{L_1(L_2+L_g)}{L_1+L_2+L_g}$$

(13)

$$C_E = \left.\frac{(R_dC_dC_fs)^2-(C_d+C_f)^2}{R_d^2C_d^2C_fs^2-(C_d+C_f)}\right|_{s=j\cdot2\pi f_{res}}$$

Substituting (13) into (11), the Q-factor at the dominant resonance frequency can be calculated. In order to analyze the relationship between the Q-factor, the damping resistor, and the grid inductance, the normalization method is adopted. The base values of the impedance, the inductance, the capacitance and the resistor can be defined as

$$Z_b=\frac{(U_g)^2}{P_o}=R_b, R_b=\sqrt{\frac{L_b}{C_b}}, C_b=\frac{1}{\omega_0 Z_b}, L_b=\frac{Z_b}{\omega_0}$$ (14)

where U_g is the RMS value of the grid voltage, ω_o is the grid frequency in rad/s and P_o is the active power generated by the inverter under rated conditions.
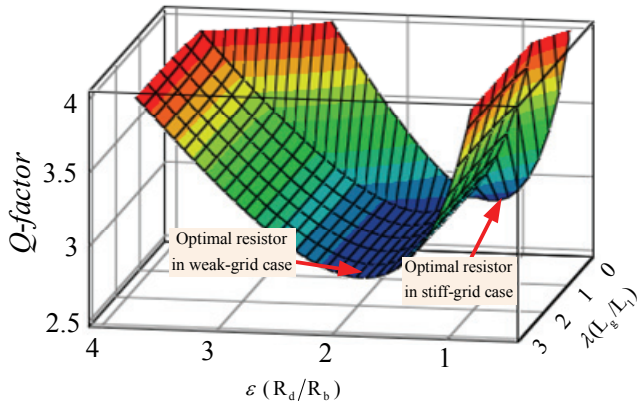

Fig. 7. *Q-factor* as a function of ε and λ for the *RC parallel* damped *LCL*-filter.

Since the R_d-C_d is paralleled with C_f, to balance the damping effect achieved and the damping losses, an equal value of C_f and C_d may be a proper selection [22]. If the discontinuous unipolar modulation mode is adopted and the current ripple ratio of L_1 is 30%, it can be derived that the converter-side inductor $L_1=0.0156L_b$. Assuming $L_2 = L_1$, $L_g = \lambda L_1$, $C_f = C_d = 0.015C_b$ and the damping resistor $R_d = \varepsilon R_b$, Q-factor as a function of ε and λ can be plotted as shown in Fig.7.

From Fig. 7 it can be seen that when the damping resistor is designed with the optimal Q-factor for a stiff grid application, the Q-factor will become large while the grid inductance increases; when the damping resistor is designed with the optimal Q-factor for a weak grid application, the Q-factor will also turn to large while the grid turns to stiffness. If the grid inductance varies in a wide range, this damping method cannot always achieve the optimal Q-factor.

From Fig.5, it can also be seen that within half of the switching frequency range, the RC parallel damped LCL-filter and $LLCL$-filter have almost the same frequency-response characteristic, if the parameters are the same except for L_f. So for an $LLCL$-filter based inverter system, E-Q-factor analysis method can also be achieved to select a reasonable damping resistor. It should be pointed that the RC parallel damped $LLCL$-filter cannot also fit for a large variation of the grid inductance [23].

C. E-Q-factor based RL series damping design

In [25], another passive damping method named as the RL series damping method for the LC-filter was introduced. In theory, this damping method is also effective for the LCL-filter as shown in Fig. 6 (a) where L_f is shortened. In this part, the design method of the exact damping parameters and the proper application of this damping method will be discussed using the E-Q-factor analysis method.

By simplifying the complex high-order circuit topologies to an equivalent series LCR circuit, the equivalent R_E and L_E of L_1, L_2, L_g and the RL series damper, can be calculated as

$$\left.\left(\frac{sL_1(\frac{sL_dR_{ds}}{sL_d+R_{ds}}+sL_2')}{sL_1+\frac{sL_dR_{ds}}{sL_d+R_{ds}}+sL_2'}\right)\right|_{s=j\omega} = R_E+sL_E$$ (15)

where $L_2'=L_2+L_g$. Then the equivalent resistor R_E, inductance L_E and capacitance C_E at the dominant resonant frequency in the series LCR circuit can be written as

$$R_E = \left.\frac{-s^2L_1^2L_d^2R_{ds}}{(L_1+L_2'+L_d)^2R_{ds}^2-s^2(L_1+L_2')^2L_d^2}\right|_{s=j\cdot2\pi f_r}$$

$$L_E = \left.\frac{L_1(L_2'+L_d)(L_1+L_2'+L_d)R_{ds}^2-s^2L_1L_2'(L_1+L_2')L_d^2}{(L_1+L_2'+L_d)^2R_{ds}^2-s^2(L_1+L_2')^2L_d^2}\right|_{s=j\cdot2\pi f_r}$$

$$C_E = C_f$$

(16)

Assuming $\delta= L_d/L_2'$, the relationship between the Q-factor, δ and η ($\eta = R_{ds}/R_b$) is plotted in Fig. 8 under the conditions that $L_1 = L_2 = 0.0156 L_b$, $C_f = 0.015 C_b$ and $L_g = 0$, which shows that the larger δ, the better Q-factor. However, a large damping inductor will increase the damping loss as well as the system cost. Since L_g is in series with L_2, an increased L_g will also result in a worsened Q-factor.
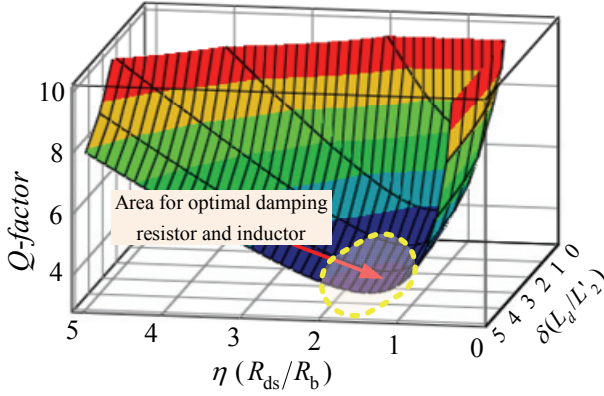
This article has been accepted for publication in a future issue of this journal, but has not been fully edited. Content may change prior to final publication.

5

Fig. 8. *Q-factor* as a function of δ and η for the *RL*- series damped *LCL*-filter.

For the *LLCL*-filter, the *RL* series damping method is also effective in theory . Compared with the *LCL*-filter, the difference is that the equivalent inductor of the *LLCL*-filter needs to be turned to (L_E+L_f). Due to the smaller grid-side inductor, both the damping inductance and the damping losses can be smaller than those of the *RL* series damped *LCL*-filter.

It should be pointed out that the *RL* series damping method is only effective in the stiff grid condition whether for an *LCL*-filter or an *LLCL*-filter.

IV. A NEW COMPOSITE PASSIVE DAMPING SCHEME FOR THE LLCL-FILTER

A. COMPOSITE PASSIVE DAMPING SCHEME

As analyzed above, for an *LLCL*-filter based system, the *RC parallel* damping method is suitable for the grid with a relatively narrow range of inductance values, while the *RL* series damping fits only for the stiff grid condition. To ensure the grid-tied inverter system stable for the grid with a wide variation range of inductance, a composite damping method for the *LLCL*-filter as shown in Fig.9 is proposed, at the expense of a little more power loss and also total inductance.
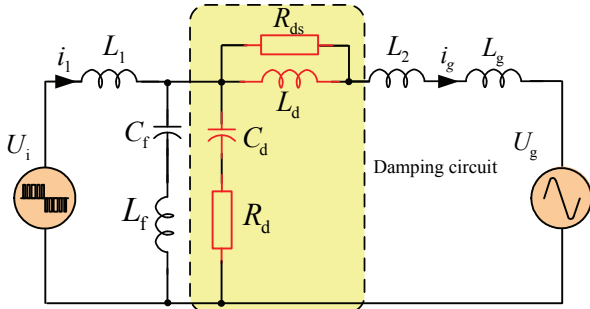

Fig. 9. Schematic diagram of the composite damping method.

The design requirements of the damping parameters can be summarized as follows,

(1) The damping resistor of R_d needs to be designed for the optimal *Q-factor* under the weakest grid condition, while C_d is equal to C_f.

(2) The damping resistor of R_{ds} is selected aiming for the optimal *Q-factor* under the stiffest grid condition, while L_d is equal to L_2.

B. DESIGN EXAMPLE

When f_s = 20 kHz, U_{dc} = 350 V, U_g = 220 V/50 Hz, P_{rated} = 2 kW, and using the discontinuous unipolar modulation mode, the main parameters of an *LLCL*-filter are designed based on the design criteria in [19], which also were listed in Table I

1) Only with *RC*-parallel damper

The *Q-factor* factor of the *RC* parallel damped *LLCL*-filter as a function of the damping resistor and the grid inductance is plotted in Fig.10when $C_d = C_f$.
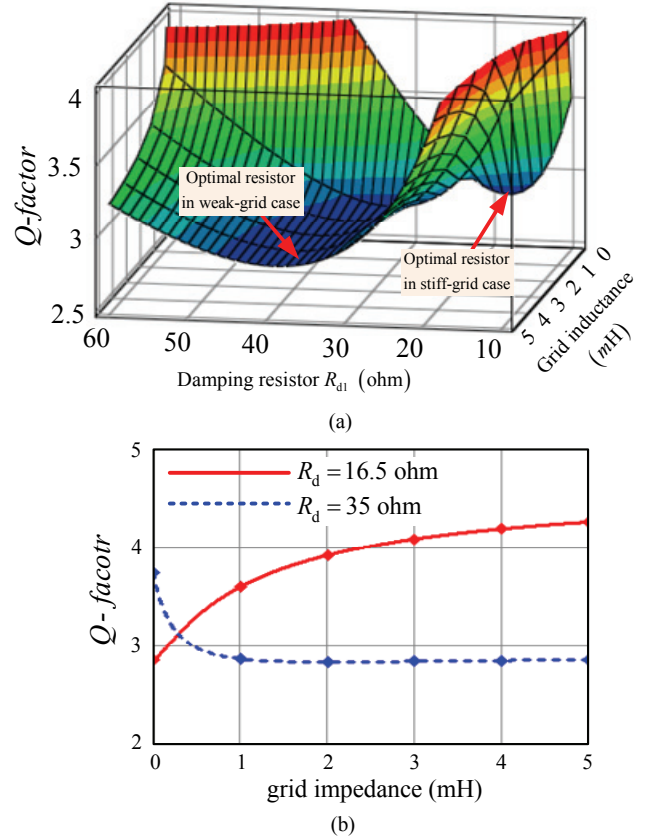

(a)

(b)

Fig. 10. Q-factor of the *RC* parallel damped *LLCL*-filter(a) Relationship between the *Q-factor*, the damping resistor and the grid inductance (b) *Q-factor* versus grid inductance, when R_d=16.5 Ω and 35 Ω.

From Fig.10 (a), it can be seen that a relatively increasing damping resistor is needed to achieve the optimal *Q-factor* with the increasing grid inductance. In order to show how the inductance variation exactly influences the *Q-factor*, Fig.10 (b) describes that the damping resistor of 16.5 Ω, which is designed for the optimal *Q-factor* under the stiff grid condition, has less damping effect with the increased inductance of the grid. On the contrary, when the damping resistor is selected to 35 Ω, which is suitable for the situation of L_g = 5 mH, the *Q-factor* becomes larger than 4 if L_g is close to 0 mH. It is difficult to select the damping resistor of the *RC* parallel damper with the optimal *Q-factor*, if the grid inductance changes in a wide range.
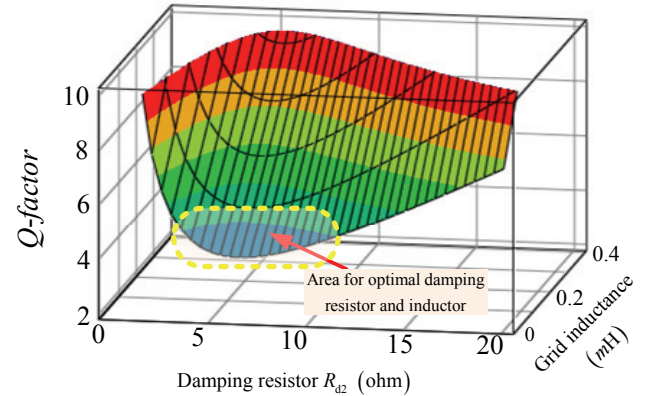

Fig.11. Relationship between the *Q-factor*, the damping resistor and the grid inductance for the *RL*- series damped *LLCL*-filter.

2) Only with *RL*- series damper

If $L_d = L_2$, the *Q-factor* as a function of the damping resistor and the grid inductance is plotted in Fig.11. It can be seen that the larger grid inductance, the larger *Q-factor* and the worse damping effect achieved. So this damping method is only effective in the stiff grid. The damping resistor can be calculated by analyzing the first-order derivative of the equivalent *Q-factor*. And a damping resistor of 7 Ω seems to achieve a good damping effect for the designed *LLCL*-filter case under the stiffest grid condition ($L_g = 0.15$ mH).
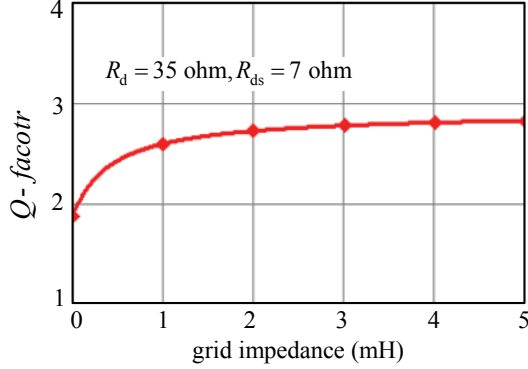

Fig.12. *Q-factor* of the composite damped *LLCL*-filter.

3) Composite passive damping scheme

For the composite damped *LLCL*-filter, when the damping parameters are selected according to the design method introduced above, it can be seen in Fig.12 that a *Q-factor* of less than 3 can be achieved in a wide variation range of grid inductance. Certainly, it should be pointed out that the stability does not just rely on the *Q-factor*, especially when the loop delay is considered. However, a small *Q-factor* does always help for the stability of the whole system.

V. ANALYSIS ON ACHIEVED DAMPING

The damping parameters of three passive-damped *LLCL*-filters can be derived and were listed in TABLE I, where the current sensor gain and the gain of PWM inverter are 0.0182 and 1400 respectively (the same as those of the experimental prototype). In order to insert the 9th harmonic compensator in the weakest grid condition ($L_g = 5$ mH), the minimum controller gain should be larger than 0.73, according to (4). With (7) and (8), k_{pmax_1} can be calculated to about 0.76 and the corresponding grid inductance is about 0.65 mH. In the real system with the digital controller, the control delay is inevitable. However, with the proper DSP control, the total delay of the system can be reduced to $0.75T_s$ [26], or less [27] (T_s is the switch period, 50μs). In this paper, the control delay is selected as $0.75T_s$. Using (10), when the phase margin is set to 45°, k_{pmax_2} can be calculated as 0.81 under the stiffest grid condition ($L_g = 0.15$ mH). Then, according to (5), the final proportional gain K_p of *PR+HC* controller is selected as 0.76, and the control bandwidth of 2.5 kHz under the stiffest grid condition and 520 Hz under the weakest grid condition can be achieved in theory.

The *PR+HC* controller is expressed as equation (17), where K_p is the proportional gain and K_{ih} represents the individual resonant integral gain.

$$G_{PR}(s) = K_p + \sum_{h=1,3,5,7,9} \frac{K_{ih}s}{s^2 + (\omega_0 h)^2} . \qquad (17)$$

In this paper, K_{ih} is selected as 100 for each harmonic compensated.

The Bode plots of the three passive-damped filters with the parameters given in Table II and the designed controller is plotted in Fig. 13. It can be seen that the system only with *RC parallel* damper (shown in Fig.13 (a)) is unstable when the grid inductance is 0.65 mH, the system with the *RL* series damper (as shown in Fig.13 (b)) is stable only under the stiff grid condition, and the system with the composite damper (shown in Fig.13 (c)) can be kept stable in a wide variation range of the grid inductance. So in terms of the acceptable system stability, the composite damping method may be the best of the three damping methods.
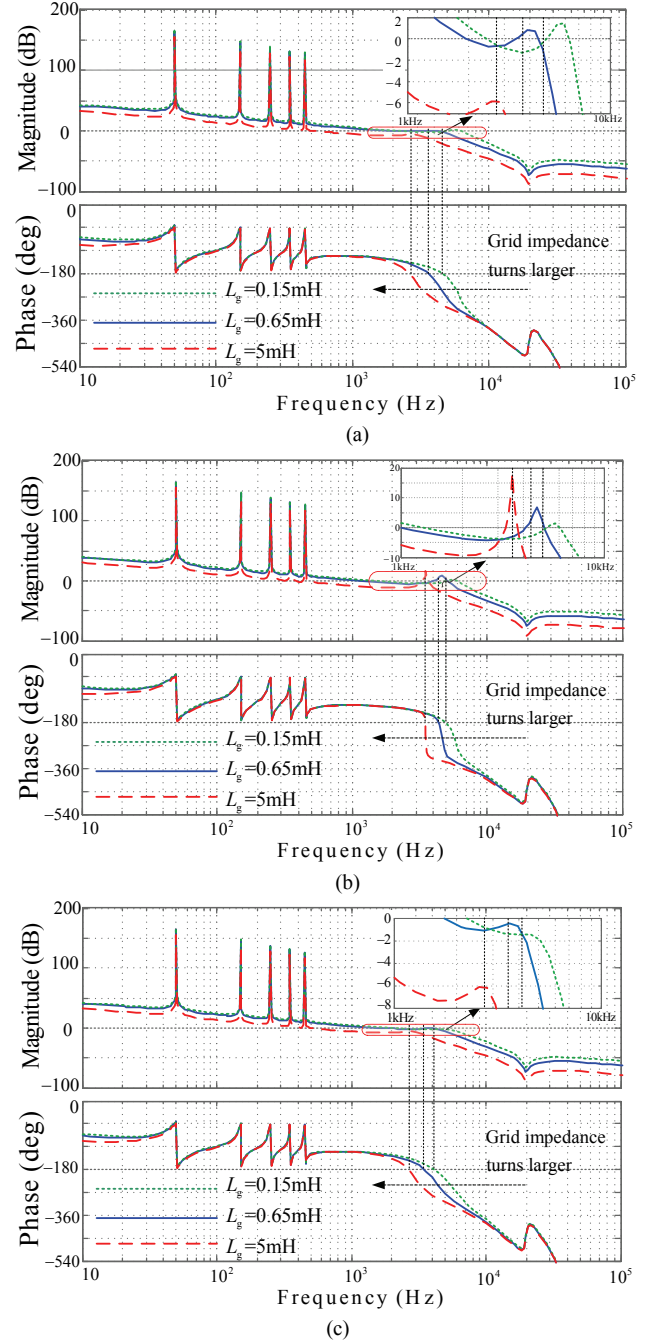

(a)

(b)

(c)

Fig. 13. Bode plots of $G_{open-loop}(j\omega)$ with the delay of 0.75 T_s for (a) Case 1: only with the *RC* parallel damper (b) Case 2: only with the *RL* series damper (c) Case 3: with the composite damper.

This article has been accepted for publication in a future issue of this journal, but has not been fully edited. Content may change prior to final publication.

7

VI.   SIMULATIONS

In order to confirm the effectiveness of the proposed damping method, simulations are carried out using the PSIM software. The parameters are the same as the designed in Table I. Referring to the design procedure developed in § III and §V, the simulations on the three cases are carried out under the given conditions that f_s = 20 kHz, U_{dc} = 350 V, U_g = 220 V/50 Hz, P_o = 2 kW, and T_d = 0.75 T_s. The current sensor gain and the gain of PWM inverter are 0.0182 and 1400 respectively for all the cases; a PR+HC (from 3rd to 9th) controller is selected for grid-current feedback controller. The parameters of the *PR+HC* controller are the same as these for analysis.
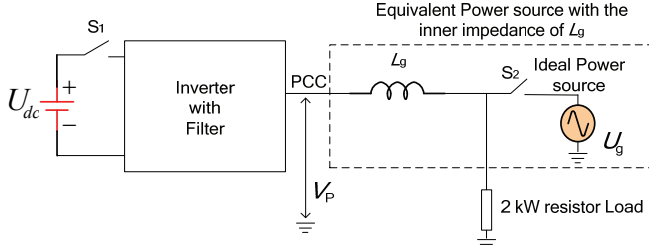

Fig. 14. System diagram for the simulations and also the experiments.

Fig. 14 shows the system diagram of for the simulations and the experiments, where the PCC is representative for the common connection point. The circuit in the dash line is used to emulate the grid with a variation of the inductance. At the time of t_0, S$_1$ switches on, and the inverter works in the off-line state. At time of t_1, S$_2$ is on, and the inverter system changes from the off-line state to the on-line state. For the simulation, it is assumed that the system begins from the off-line state directly.

When the system is stable, the simulated waveforms of the grid-injected current and the PCC voltage are similar, which are shown in Fig. 15.
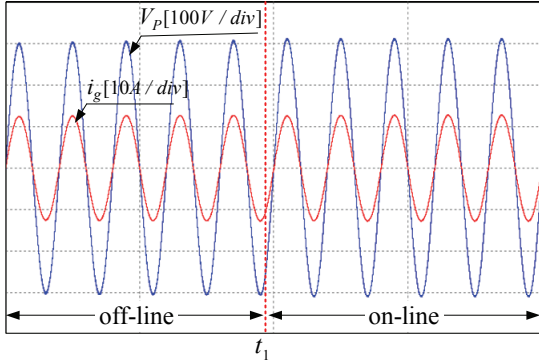

Fig. 15. Simulated grid injected currents and PCC voltages in the stable state.
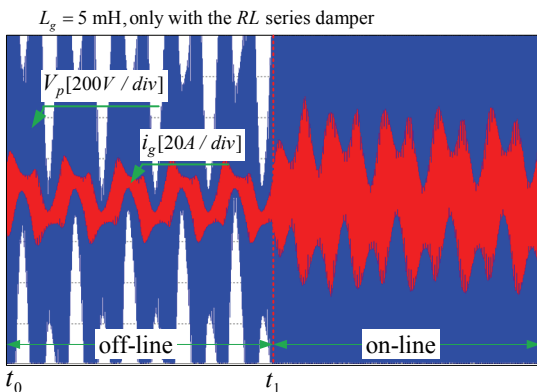

Fig. 16. Simulated grid injected currents and PCC voltages under the condition that the delay of 0.75 T_s, L_g= 5 mH, and only using the *RL* series damper.
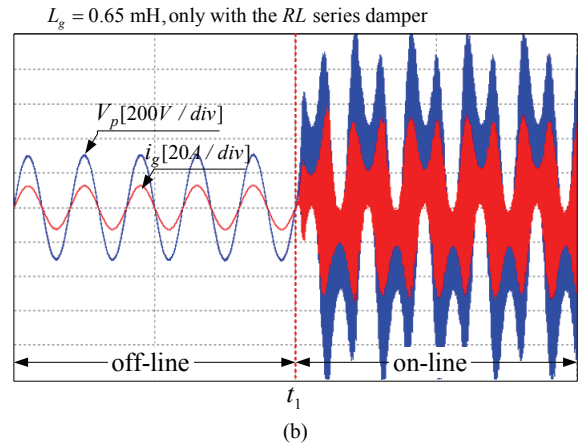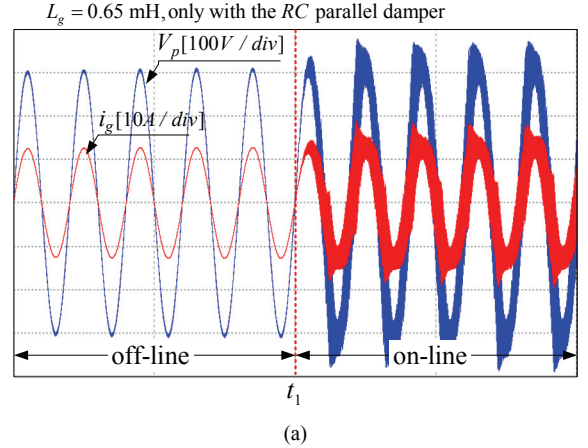

(a)

(b)

Fig. 17. Simulated grid injected currents and PCC voltages under the condition that the delay of 0.75 T_s, L_g=0.65 mH, and (a) only with the *RC* parallel damper (b) only with the *RL* series damper.

Fig. 16 shows that when L_g =5 mH, an *LLCL*-filter based system only with the *RL* series damper cannot keep stable whether it is in the off-line state or in the on-line state. Fig. 17 shows that when L_g = 0.65 mH, an *LLCL*-filter based system whether only with the *RC parallel* damper or with the *RL* series damper cannot keep stable in the on-line state. The simulations match the theoretical analysis well.

VII.   EXPERIMENTAL RESULTS

In order to further verify the theoretical analysis, a 2 kW prototype based on a DSP (TMS320LF2812) controller is constructed and the system diagram is also shown in Fig.14, where a programmable AC source (Chroma 6530) is used to emulate the ideal grid voltage. The parameters of the filters are listed in Table I and Table II, and the three different damping methods are evaluated and investigated under the given conditions that f_s = 20 kHz, U_{dc} = 350 V, U_g = 220 V/50 Hz, P_{rated} = 2 kW, the dead-time is 2 μs, and the delay is 0.75T_s.

The measured PCC voltage waveform and the grid-injected current are all similar in the stable state, which are shown in Fig. 18.

This article has been accepted for publication in a future issue of this journal, but has not been fully edited. Content may change prior to final publication.
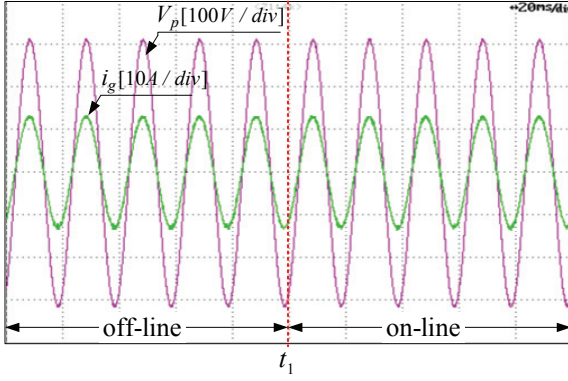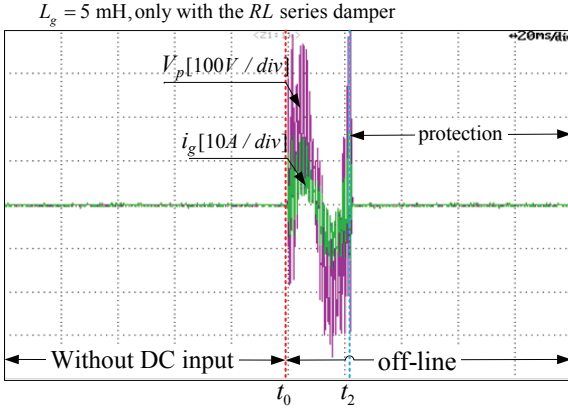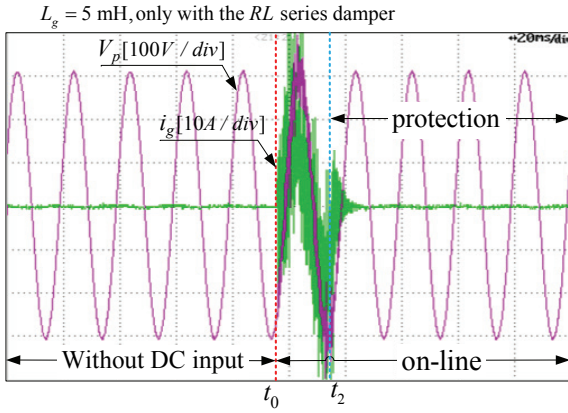
8

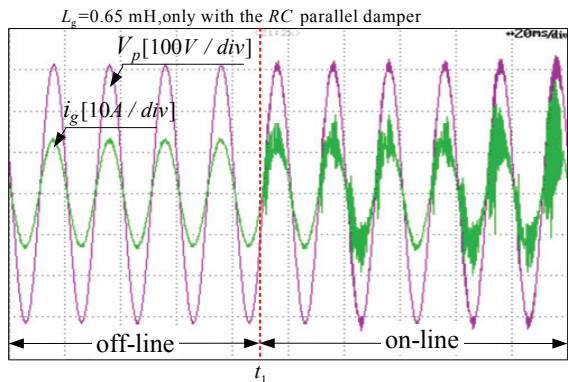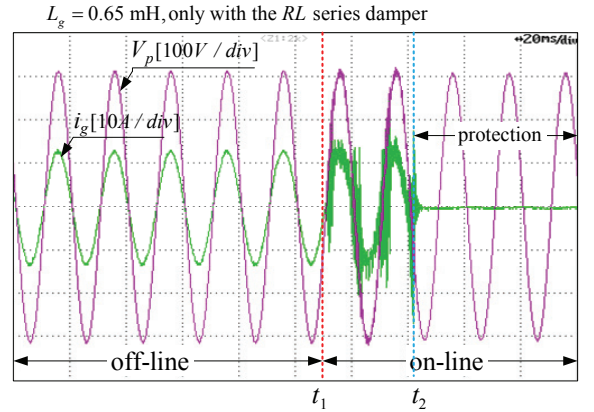Fig. 18. Measured grid-injected currents and PCC voltages in the stable state.

(a)

(b)

Fig. 19. Measured grid-injected currents and PCC voltages under the condition that the delay of 0.75 T_s, L_g= 5 mH, only with the *RL* series damper, and (a) in the off-line state (b) in the on-line state.


(a)

(b)

Fig. 20. Measured grid-injected currents and PCC voltages under the condition that the delay of 0.75 T_s, L_g= 0.65 mH, and (a) Only with the *RC* parallel damper (b) Only with the *RL* series damper.

Fig. 19 shows the experimental results under the weak grid conditions of L_g= 5 mH and the delay of 0.75 T_s, showing that the *RL* series damped system cannot keep stable whether in the off-line state or in the on-line state. It can also be seen that due to the resonance, the over currents trigger the hardware protections at the time of t_2. Note that due to hardware protection, the state transition (from the off-line to the on-line at the time of t_1) of the *RL* series damped system cannot be observed directly. As shown in Fig. 19(a) and Fig. 19 (b), the resonances in the on-line and off-line states are observed with the help of the switch S_1 which is switching on at the time of t_0.
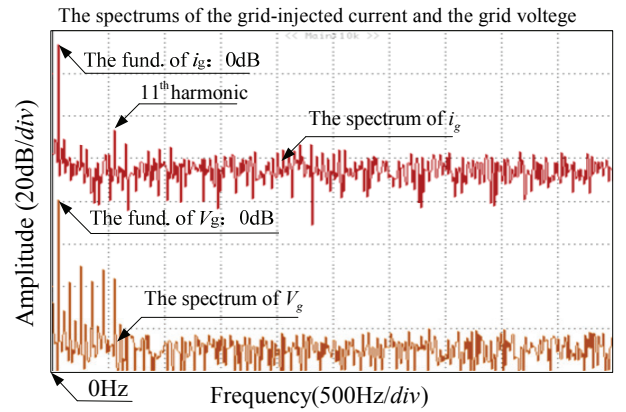
Fig. 20 shows that when L_g =0.65 mH, an *LLCL*-filter based system whether only with the *RC* parallel or with the *RL* series damper cannot keep stable in the on-line state.
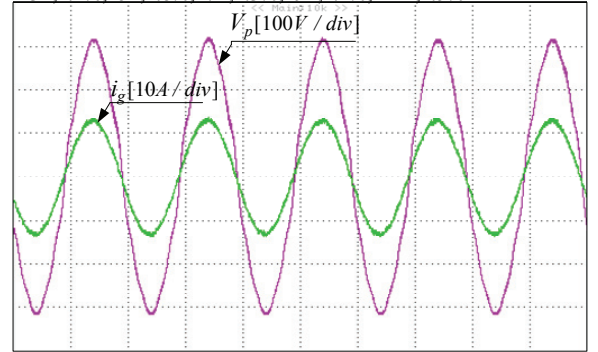
(a)

(b)

Fig. 21. Measured grid injected current and grid voltage under the condition that the delay of 0.75 T_s, L_g= 5 mH, and the composite damper is

This article has been accepted for publication in a future issue of this journal, but has not been fully edited. Content may change prior to final publication.

9

adopted (a) Grid-injected current and the distorted grid voltage (b) Spectra of the grid-injected current and the grid voltage.

Fig. 21 (a) shows the measured grid-injected current and the grid voltage of the composite damping *LLCL*-filter based grid tied inverter under the condition that L_g= 5 mH and the magnitudes of the injected 3th, 5th, 7th, 9th and 11th harmonics with respect to the fundamental component of U_g are 1.2%, 2.8%, 1.3%, 2.4%, and 1.5%, respectively. Fig. 21 (b) shows the spectra of the grid-injected current and the grid voltage. Since the harmonics compensation of 3th, 5th, 7th and 9th are adopted, the related harmonic currents are well suppressed, while the 11th harmonic current cannot be alleviated.

The experimental results shows that under the same condition of the grid with the large variation of inductance, the control robust of the system with the composite damper is improved a lot, compared with the system only with the *RC* parallel damper or with the *RL* series damper. The experiment matches the theoretical analysis and the simulations quite well.

VIII. CONCLUSION

This paper has discussed the passive damping design for a high order power filter based grid-tied inverter. The following can be concluded.

1. The *RC parallel* damping method can be adopted for the system under the condition of the weak grid or the stiff grid, but is only suitable for the grid with a narrow variation of inductance.
2. The *RL* series passive damping method is only useful for the system under the stiff grid condition.
3. A robust passive damping method for the *LLCL*-filter based inverter connected to a grid with a large variation of inductance can be achieved with a composite passive damper, where its *RC parallel* part is designed under the weakest grid condition while its *RL* series part is designed under the stiffest grid condition, certainly at little more cost of materials and power losses.
4. The proposed damping method may only be suitable for the *LLCL*-filter based system, due to the additional power losses and inductance.

The effectiveness of the proposed damping method is fully verified through the simulations and experiments on a 2 kW *LLCL*-filter based single–phase grid-tied inverter prototype with the fixed controller gain, while the grid inductance varies from 0.15 mH to 5 mH.

ACKNOWLEDGEMENTS

REFERENCES

[1] Liserre, M.; Blaabjerg, F.; Hansen, S., "Design and control of an LCL-filter-based three-phase active rectifier," *Industry Applications, IEEE Transactions on* , vol.41, no.5, pp.1281,1291, Sept.-Oct. 2005.
[2] Y. A.-R. I. Mohamed, M.A.-Rahman, R. Seethapathy, "Robust Line-Voltage Sensorless Control and Synchronization of LCL - Filtered Distributed Generation Inverters for High Power Quality Grid Connection," *IEEE Trans. Power Electron*., vol.27, no.1, pp.87-98, Jan. 2012.
[3] Y. Tang, P. Loh, P. Wang, F. Choo, F. Gao, "Exploring Inherent Damping Characteristic of LCLFilters for Three-Phase Grid-Connected Voltage Source Inverters," Power Electronics, *IEEE Trans. Power Electron.*, vol.27, no.3, pp.1433-1443, March 2012.
[4] J. L. Agorreta, M. Borrega, J. López, and L. Marroyo, "Modeling and Control of N-Paralleled Grid-Connected Inverters With *LCL* Filter Coupled Due to Grid Impedance in PV Plants," *IEEE Trans. Power Electron.*,vol.26, no.3, pp.770-785, March 2011.
[5] Zhang, Y. M. Xue, Y. Kang, Y. Yi, S. Li, F. Liu, "Full Feedforward of Grid Voltage for Discrete State Feedback Controlled Grid-Connected Inverter With LCL Filter," Power Electronics, *IEEE Trans. Power Electron.*, vol.27, no.10, pp.4234-4247, Oct. 2012.
[6] J. He, Y. W. Li, "Generalized Closed-Loop Control Schemes with Embedded Virtual Impedances for Voltage Source Converters with LC or LCL Filters," *IEEE Trans. Power Electron.*, vol.27, no.4, pp.1850-1861, April 2012.
[7] X. Hao, X. Yang, T. Liu, L. Huang, W. Chen, "A Sliding-Mode Controller With Multiresonant Sliding Surface for Single-Phase Grid-Connected VSI With an LCL Filter," *Power Electronics*, *IEEE Transactions on*, vol.28, no.5, pp.2259-2268, May 2013.
[8] R. Peña-Alzola, M. Liserre, F. Blaabjerg, R. Sebastián, J. Dannehl, F.W. Fuchs, "Analysis of the Passive Damping Losses in LCL-Filter-Based Grid Converters," *Power Electronics*, *IEEE Transactions on*, vol.28, no.6, pp. 2642-2646, June 2013.
[9] X. Bao, F. Zhuo, Y. Tian, P. Tan, "Simplified Feedback Linearization Control of Three-Phase Photovoltaic Inverter With an LCL Filter," *Power Electronics*, *IEEE Transactions on*, vol.28, no.6, pp. 2739-2752, June 2013.
[10] N. He, D. Xu, Y. Zhu, J. Zhang, G. Shen, Y. Zhang, J. Ma; C. Liu, "Weighted Average Current Control in a Three-Phase Grid Inverter With an LCL Filter," *Power Electronics*, *IEEE Transactions on*, vol.28, no.6, pp. 2785-2797, June 2013.
[11] J. Mulethaler, M. Schweizer, R. Blattmann, J.W. Kolar, A. Ecklebe, "Optimal Design of LCL Harmonic Filters for Three-Phase PFC Rectifiers," *Power Electronics*, *IEEE Transactions on*, vol.28, no.7, pp. 3114-3125, Jul. 2013.
[12] A. Kulkarni, V. John, "Mitigation of Lower Order Harmonics in a Grid-Connected Single-Phase PV Inverter," *Power Electronics*, *IEEE Transactions on*, vol.28, no.11, pp. 5024-5037, Nov. 2013.
[13] M. Hartmann, H. Ertl, J.W. Kolar,"Current Control of Three-Phase Rectifier Systems Using Three Independent Current Controllers," *Power Electronics*, *IEEE Transactions on*, vol.28, no.8, pp. 3988-4000, Aug. 2013.
[14] B.J. Pierquet, D.J. Perreault,"A Single-Phase Photovoltaic Inverter Topology With a Series-Connected Energy Buffer," *Power Electronics*, *IEEE Transactions on*, vol.28, no.10, pp. 4603-4611, Oct. 2013.
[15] T.S. Hwang, S.Y. Park, "A Seamless Control Strategy of a Distributed Generation Inverter for the Critical Load Safety Under Strict Grid Distrubances," *Power Electronics*, *IEEE Transactions on*, vol.28, no.10, pp. 4780-4790, Oct. 2013.
[16] *IEEE Application Guide for IEEE Std. 1547, IEEE Standard for Interconnecting Distributed Resources With Electric Power Systems*, IEEE 1547.2-2008, 2008.
[17] *IEEE Recommended Practices and Requirements for Harmonic Control in Electrical Power Systems*, IEEE 519-1992, 1992.
[18] M. Lindgren and J. Svensson, "Connecting Fast Switching Voltage Source Converters to the Grid—Harmonic Distortion and its Reduction", *in Proc. of IEEE Stockholm Power Tech. Conf.*, Stockholm, Sweden, pp. 191-196, June 18-22, 1995.
[19] W. Wu, Y. He, and F. Blaabjerg, "An *LLCL-* Power Filter for Single-phase Grid-tied Inverter," *IEEE Trans. Power Electron.,* vol. 27, no. 2, pp. 782-789, Feb. 2012.
[20] M. Liserre, R. Teodorescu, and F. Blaabjerg, "Stability of photovoltaic and wind turbine grid-connected inverters for a large set of grid impedance values", *IEEE Trans. Power Electron.,* vol. 21, no. 1, pp. 263–272, Jan. 2006.
[21] J. R. Massing, M. Stefanello, H. A. Gründling, and H. Pinheiro, Adaptive Current Control for Grid-Connected Converters With LCL

This article has been accepted for publication in a future issue of this journal, but has not been fully edited. Content may change prior to final publication.

10

Filter, *IEEE Trans. Ind. Electron.,* vol. 59, no. 12, pp. 4681-4693, Dec. 2012.

[22] P. Channegowda and V. John, "Filter Optimization for Grid Interactive Voltage Source Inverters", *IEEE Trans. Ind. Electron.,* vol. 57, no. 12, pp. 4106–4114, Dec. 2010.

[23] W. Wu, Y. He, and F. Blaabjerg, "A New Design Method for the Passive Damped LCL- and LLCL-Filter Based Single-Phase Grid-tied Inverter", *IEEE Trans. Ind. Electron.,*vol. 60, no. 10, pp. 4339-4350, Oct. 2013.

[24] X. Yuan, W. Merk, H. Stemmler, J. Allmeling – "Stationary-Frame Generalized Integrators for Current Control of Active Power Filters with Zero Steady-State Error for Current Harmonics of Concern Under Unbalanced and Distorted Operating Conditions", *IEEE Trans. Ind. App.,* vol. 38, no. 2, pp.523 – 532, Mar./Apr. 2002.

[25] L. Xing, F. Feng, and J. Sun, "Optimal Damping of EMI Filter Input Impedance", *IEEE Tran. Ind. App.,* vol.47, no.3, pp.1432-1440, May-June 2011.

[26] S. A. S. Grogan, D. G. Holmes, and B. P. McGrath, "High-performance voltage regulation of current source inverters," *IEEE Trans. Power Electron.,* vol. 26, no. 9, pp. 2439–2448, Sept. 2011.

[27] L. Corradini, W. Stefanutti, and P. Mattavelli, "Analysis of Multisampled Current Control for Active Filters," *IEEE Trans. Ind. App.,* vol.44, no.6, pp.1785-1794, Nov.-Dec. 2008.

Weimin Wu received the B.S. degrees from the Department of Electrical Engineering, Anhui University of Science & Technology, Huainan, China, in 1997, M.S. degrees from the Department of Electrical Engineering, Shanghai University, Shanghai, China, in 2001, and Ph.D. degrees from the College of Electrical Engineering, Zhejiang University, Hangzhou, China, in 2005.

He worked as a research engineer in Delta Power Electronic Center (DPEC), Shanghai, from July, 2005 to June, 2006. Since July, 2006, he has been a Faculty Member at Shanghai Maritime University, where he is currently an Associate Professor in the Department of Electrical Engineering. He was a Visiting Professor in the Center for Power Electronics Systems (CPES), Virginia Polytechnic Institute and State University, Blacksburg, from Sept. 2008 to March. 2009. From Nov. 2011 to Jan. 2014, he is also a visiting professor in the Department of Energy Technology, working at the Center of Reliable Power Electronics (CORPE). He has coauthored about 40 papers in technical journals and conferences. He is the holder of three patents. His areas of interests include power converters for renewable energy systems, power quality, smart grid, and energy storage technology.

Yunjie Sun was born in Heilongjiang Province, China, in 1988. He received the B.S. and M.S. degrees from the Department of Electrical Engineering, Shanghai Maritime University, Shanghai, China, in 2011 and 2013, respectively.

He is currently working in Action-Power Co., Ltd., Xi'an, China. His current research interests include digital control technique, power quality compensator and renewable energy generation system.

Min Huang was born in Hunan Province, China, in 1988. She received the B.S. degree from the Department of Electrical Engineering, Shanghai Maritime University, Shanghai, China. She is currently working toward the Ph.D.degree in the Institute of Energy Technology, Aalborg University, Aalborg, Denmark.

Her research interests include power quality, control and power converters for renewable energy systems .
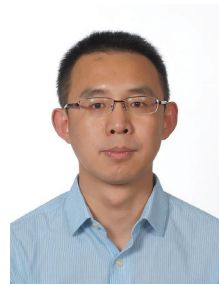
Xiongfei Wang (S'2010-M'2013) received the B.Sc. degree from Yanshan University, Qinhuangdao, China, in 2006 and the M.Sc. degree from Harbin Institute of Technology, Harbin, China, in 2008, both in electrical engineering, and the Ph.D. degree in energy technology from Aalborg University, Aalborg, Denmark in 2013. He was a visiting student at Hanyang University, Seoul, South Korea, from 2007 to 2008.

Since 2009, he has been with the Aalborg University, Aalborg, Denmark, where he is currently a Post Doc in the Department of Energy Technology. His research areas are in the power electronics for renewable energy systems, distributed generations, microgrids, and power quality issues.
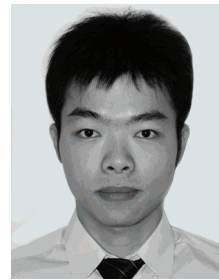
Huai Wang (S'07 - M'12) received the B.Eng. Degree in Electrical and Electronic Engineering from Huazhong University of Science and Technology, Wuhan, China, in 2007, and the Ph.D. degree in Electronic Engineering from City University of Hong Kong, Kowloon, Hong Kong, in 2012.

Since 2012, he has been with Aalborg University, Denmark, where he is currently an Assistant Professor in the Department of Energy Technology, working at the Center of Reliable Power Electronics (CORPE). From April to September 2010, he was an intern student at ABB Corporate Research Center, Switzerland. From November 2007 to December 2008, he was a research assistant at the Centre for Power Electronics (CPE), City University of Hong Kong. He has authored or coauthored more than 30 technical papers and filed 3 patents. His research interests include reliability of capacitors for dc-link application, reliability of power electronic systems, high-voltage dc-dc power converters, fast dynamic control of converters, and passive components reduction technology.

Frede Blaabjerg (S'86–M'88–SM'97–F'03) was with ABB-Scandia, Randers, Denmark, from 1987 to 1988. From 1988 to 1992, he was a Ph.D. Student with Aalborg University, Aalborg, Denmark. He became an Assistant Professor in 1992, an Associate Professor in 1996, and a Full Professor of power electronics and drives in 1998. He has been a part time Research Leader with the Research Center Risoe in wind turbines. From 2006 to 2010, he was the Dean of the Faculty of Engineering, Science, and Medicine and became a Visiting Professor with Zhejiang University, Hangzhou, China, in 2009. His current research interests include power electronics and its applications such as in wind turbines, PV systems, reliability, harmonics and adjustable speed drives.

He received the 1995 Angelos Award for his contribution in modulation technique and the Annual Teacher Prize at Aalborg University. In 1998, he received the Outstanding Young Power Electronics Engineer Award by the IEEE Power Electronics Society. He has received 14 IEEE Prize Paper Awards and another Prize Paper Award at PELINCEC Poland in 2005. He received the IEEE PELS Distinguished Service Award in 2009, the EPE-PEMC Council Award in 2010 and the IEEE William E. Newell Power Electronics Award 2014. He has received a number of major research awards in Denmark. He was an Editor-in-Chief of the IEEE TRANSACTIONS ON POWER ELECTRONICS from 2006 to 2012. He was a Distinguished Lecturer for the IEEE Power Electronics Society from 2005 to 2007 and for the IEEE Industry Applications Society from

2010 to 2011. He was a Chairman of EPE in 2007 and PEDG,

Marco Liserre (S'00-M'02-SM'07-F'13) . He received the MSc and PhD degree in Electrical Engineering from the Bari Polytechnic, respectively in 1998 and 2002. From 2004 he was Assistant Professor, and from 2012 Associate Professor at Bari Polytechnic. He is Professor in reliable power electronics at Aalborg University (Denmark). He has published 162 technical papers (40 of them in international peer-reviewed journals, of which 19 in the last five years 2007-2011), 3 chapters of a book and a book (Grid Converters for Photovoltaic and Wind Power Systems, ISBN-10: 0-470-05751-3 – IEEE-Wiley, also translated in Chinese). These works have received more than 4000 citations. He has been visiting Professor at Alcala de Henares University (Spain) and at Christian-Albrechts University of Kiel, Germany, as Mercator professor.

He is member of IAS, PELS, PES and IES. He is Associate Editor of the IEEE Transactions on Industrial Electronics, IEEE Industrial Electronics Magazine, IEEE Transactions on Industrial Informatics, IEEE Transactions on power electronics and IEEE Transactions on sustainable energy. He has been Founder and Editor-in-Chief of the IEEE Industrial Electronics Magazine, Founder and the Chairman of the Technical Committee on Renewable Energy Systems, Co-Chairman of the International Symposium on Industrial Electronics (ISIE 2010), IES Vice-President responsible of the publications. He has received the IES 2009 Early Career Award, the

Aalborg, in 2012.

IES 2011 Anthony J. Hornfeck Service Award and the 2011 Industrial Electronics Magazine best paper award. He is a senior member of IES AdCom. He has been elevated to the IEEE fellow grade with the following citation "for contributions to grid connection of renewable energy systems and industrial drives".

Henry Shu-hung Chung ('95 M, '03SM) received his B.Eng. degree in 1991 and PhD degree in 1994 in electrical engineering, both from The Hong Kong Polytechnic University. Since 1995 he has been with the City University of Hong Kong (CityU). He is currently professor of the Department of Electronic Engineering, and Director of the Centre for Smart Energy Conversion and Utilization Research. His research interests include time- and frequency-domain analysis of power electronic circuits, switched-capacitor-based converters, random-switching techniques, control methods, digital audio amplifiers, soft-switching converters, and electronic ballast design. He has authored six research book chapters, and over 300 technical papers including 140 refereed journal papers in his research areas, and holds 26 patents. Dr. Chung is currently Chairman of Technical Committee on High-Performance and Emerging Technologies of the IEEE Power Electronics Society, and Associate Editor of the IEEE Transactions on Power Electronics, IEEE Transactions on Circuits and Systems, Part I: Fundamental Theory and Applications, and IEEE Journal of Emerging and Selected Topics in Power Electronics.